

Wind-induced single-sided natural ventilation in buildings near a long street canyon: CFD evaluation of street configuration and envelope design

Z.T. Ai

(a) Department of Building Services Engineering, The Hong Kong Polytechnic University, Hong Kong

(b) International Centre for Indoor Environment and Energy, Department of Civil Engineering, Technical University of Denmark

E-Mail: zhengtao.ai@connect.polyu.hk; zheai@byg.dtu.dk

C.M. Mak (Corresponding author)

Department of Building Services Engineering, The Hong Kong Polytechnic University, Hong Kong

Tel.: +852 2766 5856; Fax: +852 2765 7198

E-Mail: cheuk-ming.mak@polyu.edu.hk

Abstract: Wind-induced single-sided natural ventilation in buildings was widely investigated based on isolated buildings. However, owing to the presence of surrounding buildings, the wind flow pattern around a building in an urban area becomes very different from that around an isolated building. Considering an urban context, this study investigates the wind-induced single-sided natural ventilation in buildings near a long street canyon under a perpendicular wind direction using CFD method. Four aspect ratios (AR) of the street canyon, from 1.0, 2.0, 4.0 to 6.0, are investigated to examine the influence of street configuration, while eight envelope features are compared to explore the possibility of envelope design in improving natural ventilation performance of urban buildings. Ventilation rate of rooms in buildings is particularly analyzed. AR influences ventilation rate and its distribution among rooms along height of buildings. The percentage decrease of ventilation rate of buildings reaches 67% when AR of a street canyon is increased from 1.0 to 6.0. Envelope design provides a possibility to enhance the adaptability of buildings to dense urban environments. A good envelope design, such as a horizontal feature at the middle of an opening, can break effectively the along-facade flow and thus create a large pressure difference to drive ventilation. The findings of this study are intended to increase the understanding of natural ventilation performance in urban buildings and thus provide information for urban planning and building design.

Keywords: Natural ventilation, urban environment, street canyon, envelope design, CFD simulation

1. Introduction

Natural ventilation is widely existed in urban buildings intentionally or unintentionally. It is intentionally designed to create a healthy and thermally comfortable indoor environment by utilizing optimally the driving force of wind and buoyancy effects, when the outdoor microclimate environment is desirable. In many buildings including particularly residential buildings, window(s) are not necessarily opened for obtaining natural ventilation, but natural ventilation is certainly formed in such situations. Regardless of intentions, the wide existence of natural ventilation in urban buildings is worthy of a special attention, considering that the indoor environmental quality in these naturally ventilated buildings is strongly influenced by their nearby urban microclimate (Ai and Mak, 2015).

Compared to cross natural ventilation, single-sided natural ventilation is much more common in buildings, especially in densely populated urban areas where many rooms are characterized by a single window and a closed door. While buoyancy effect is an important driving force of natural ventilation in buildings where there are large differences in both indoor/outdoor air temperature and vertical distance of intake and exhaust openings, wind effect is normally the dominated driving force for natural ventilation in most buildings like residential buildings. Wind-driven single-sided natural

ventilation is a complex process that is influenced by the turbulent nature of the approaching wind and the bi-directional airflow interaction at the opening (Haghighat et al., 1991, 2000; Linden, 1999; Ai and Mak, 2014a). Single-sided natural ventilation can be predicted by empirical models (Warren, 1977; Phaff and De Gids, 1982; Larsen and Heiselberg, 2008; Wang and Chen, 2012), experimental measurements (Caciolo et al., 2011; Dascalaki et al., 1996; Karava et al., 2011), and computational fluid dynamics (CFD) models (Jiang and Chen, 2001; Caciolo et al., 2012; Ai et al., 2013; 2016; van Hooff and Blocken, 2010). Compared with the first two approaches, CFD simulation has some advantages for the study of single-sided natural ventilation that involves coupled urban wind flow and indoor air flow (van Hooff and Blocken, 2010; Blocken and Gualtieri, 2012; Ai and Mak, 2014a). These previous studies are very useful in revealing basic flow behaviours, examining parameters and validating CFD models, which, however, are mostly limited to isolated buildings, such as a single-room building (e.g., Jiang et al., 2001; Straw, 2000; Ai and Mak, 2014a) and a multiple-room building (e.g., Ai et al., 2013; Ai and Mak, 2016).

Given that few buildings in urban areas can be regarded as isolated buildings, the urban microclimate would directly influence the natural ventilation in buildings. Studies in urban physics and wind engineering indicate that wind speed in a street canyon flanked by buildings is decreased significantly compared to that above the canyon (Oke, 1987; HKPD, 2005; Georgakis and Santamouris, 2006). Depending on aspect ratio (AR, ratio of the mean building height to the street width) (Oke, 1987; Li et al., 2006; Ai and Mak, 2015), flow pattern in a street canyon can be categorized into three regimes: isolated roughness flow ($AR < 0.3-0.4$), wake interference flow ($0.3-0.4 < AR < 0.65-0.7$) and skimming flow ($AR > 0.65-0.7$). The study of atmospheric processes in skimming-flow street canyons were paid particular attentions, as they are considered to be with the worst flow and dispersion conditions when compared to those in lower AR streets. Review of on-site measurements (Georgakis and Santamouris, 2006; Andreou and Axarli, 2012; Nakamura and Oke, 1988; Santamouris et al., 1999; Manning et al., 2000; Buller, 1976; Niachou et al., 2008; Kitous et al., 2012) of wind speeds inside and outside (mostly above) street canyons by Ai and Mak (2015) suggests that, depending on AR, the ratio of wind speed inside a canyon to that outside the canyon ranges mostly between 10% and 30%. The review (Ai and Mak, 2015) also shows that wind direction in vicinity of a building near a street canyon is dominated by the along canyon flow combined with upward and downward movements, while the normal-to-facade flows are very weak. The decreased wind speeds and substantially changed flow patterns inside street canyons would influence (mostly lower) wind-induced pressure difference for natural ventilation in buildings, which thus highlight the importance of taking into account urban context in natural ventilation studies.

On-site measurement of natural ventilation rate (Georgakis and Santamouris, 2006; Gilkeson et al., 2013; Li et al., 2014; Santamouris et al., 2008) is a useful method to reveal the real-life ventilation performance of naturally ventilated buildings in urban areas. However, since the natural ventilation rate is influence by many factors, such as wind speed and direction, opening configuration, surrounding characteristics and floor location in a building, these measured results vary significantly between different cases and over time, which are thus cannot provide a general view on the influence of surrounding buildings on natural ventilation performance. A few studies examined the natural ventilation performance in buildings when considering the influence of surrounding buildings, which show that the wind speed near building facades could be lowered by up to 86.8% (Gao and Lee, 2012) and the natural ventilation performance in urban buildings could drop by up to 96% (van Hooff and Blocken, 2010; Georgakis and Santamouris, 2006) when compared to isolated buildings. These findings are, however, case dependent and again may not be applicable to a different situation.

In general, current understanding of natural ventilation in urban buildings is far from sufficient, and there is still a strong need to provide a systematical investigation using a general urban geometry. From both street configuration and envelope design perspectives, the objective of this study is to

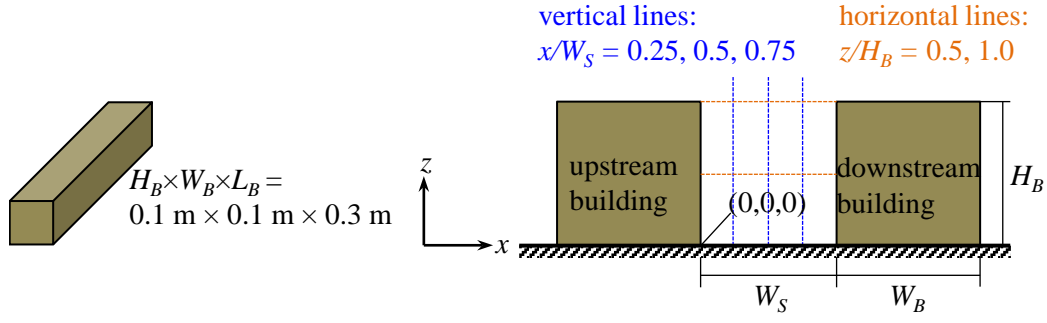
investigate the wind-induced single-sided natural ventilation in urban buildings. A long street canyon flanked by two buildings is considered, while four AR values are investigated, including 1.0, 2.0, 4.0 and 6.0, which all correspond to the aforementioned skimming flow regime (Oke, 1987; Ai and Mak, 2015). Based on the four AR values, eight envelope features are examined to explore the possibility of improving the natural ventilation performance of urban buildings through envelope design. Each of the two buildings contains 11 floors and 23 rooms on each floor. As the street canyon is considered to be ideally infinitely long, only the rooms located on the vertical centres are created for investigation. Ventilation performance of rooms is particularly evaluated using air change rate per hour (ACH). CFD simulations are conducted and steady-state results are obtained by solving the Reynolds-Averaged Navier-Stokes (RANS) equations using the Renormalization group (RNG) $k-\varepsilon$ turbulence model. The rationality and limitation of such steady-state simulations are discussed in Section 5. CFD model is validated first to ensure its reliability (Section 2). Section 3 describes in detail the investigated street canyons, buildings and envelope features as well as computational settings. Section 4 presents results and analyses, Section 5 discussions and Section 6 conclusions.

2. CFD simulations: model validation

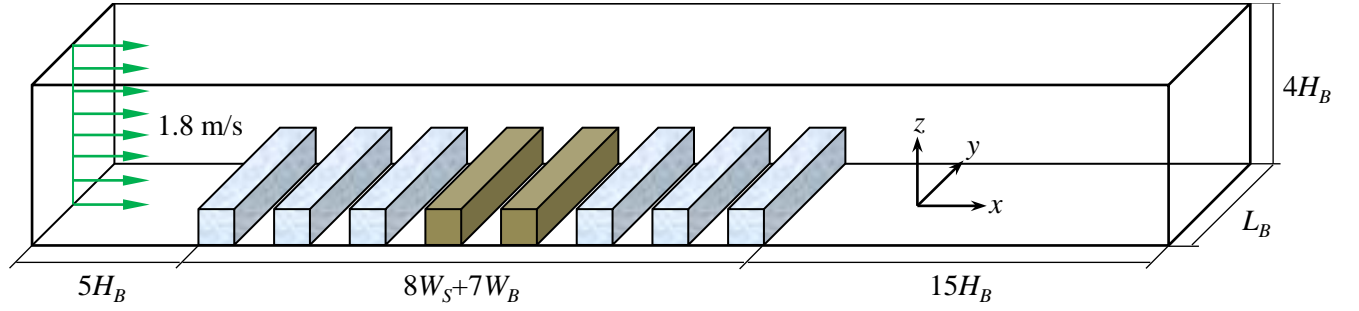
Model validation against experimental data is a basic requirement to ensure the reliability of any CFD simulations. Natural ventilation in buildings near a street canyon investigated in this study involves two elementary flow problems: (a) single-sided natural ventilation that includes a coupled indoor and outdoor flow field, and (b) street canyon flow that includes the interaction between the flows inside and above the street canyon. It is necessary to validate the two elementary flow problems. However, an experiment involving both the two flow problems is rarely found in previous literature. In this study, the two flow problems were validated separately using different experiments. First, for single-sided natural ventilation in buildings, a wind tunnel experiment by Jiang et al. (2003) and a field experiment by Dascalaki et al. (1996) were employed to conduct validations. Detailed validation processes and comparisons between the simulated results and the experimental data can be found in our previous papers (Ai et al., 2013; Ai and Mak, 2014a,b). In general, both the predicted flow field (Jiang et al., 2003; Ai et al., 2013; Ai and Mak, 2014a) and ACH value (Dascalaki et al., 1996; Ai and Mak, 2014a) show an acceptable agreement with the measured data. These comparisons justified the use of our CFD model in the prediction of single-sided natural ventilation in buildings. Second, for street canyon flow, a water tunnel experiment by Li et al. (2008a) was used. The detailed description of this validation is presented in the following Sections 2.1-2.3.

2.1. Validation of street canyon flow

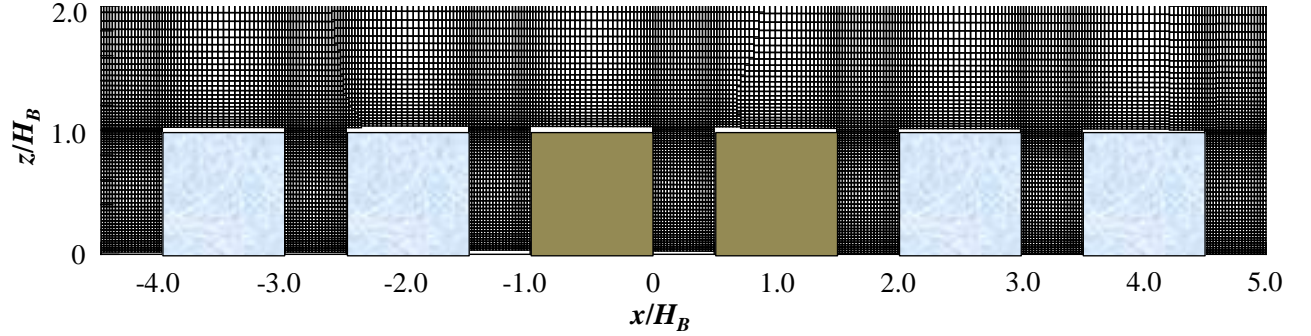
Li et al. (2008a) conducted a water tunnel ($L_T \times W_T \times H_T$: 10 m \times 0.3 m \times 0.5 m) experiment to measure the flow field inside a street canyon. Two types of street canyons of AR (H_B/W_S) equal to 1.0 and 2.0 were investigated, which were formed by eight and ten identical building models ($L_B \times W_B \times H_B$: 0.3 m \times 0.1 m \times 0.1 m), respectively. The water flow approaches the street canyons in a perpendicular direction (Figure 1 (b)). The height of the buildings was fixed at $H_B = 0.1$ m, while the width of the street canyons W_S was varied to form the two AR values. The depth of water in the two sets of experiments was fixed at 0.4 m. The Reynolds number based on the reference water speed (U_{ref}) in freestream at $z = 0.3$ m and the building height was 12,000, implying that U_{ref} was equal to 1.8 m/s. No roughness elements on the tunnel ground were considered. Velocity components in the streamwise and vertical directions along three vertical lines and two horizontal lines on the vertical centerplane ($y = 0$) of the target street canyon (see Figure 1 (a)) were measured using a two-colour laser Doppler anemometer (LDA).



(a) building model and the vertical centerplane ($y = 0$) of the target street canyon model



(b) computational domain



(c) mesh information on part of vertical centerplane ($AR = 2$)

Figure 1 The street canyon model, computational domain and mesh information.

The building model and street canyon model used in CFD simulations are the same with those in the experiments (see Figure 1 (a) and (b)). Computational domain and its dimensions (see Figure 1 (b)) are selected based on the existing best practice guidelines for CFD simulation of urban aerodynamics (Franke et al., 2007; Tominaga et al., 2008), except that the height and lateral length of the domain follow those in the experiments. The whole computational domain is constructed using structured hexahedral cells (see Figure 1 (c)). After a grid sensitivity test, two grids, with 3,168,000 and 2,880,000 cells in total, are eventually used for the cases of $AR = 1.0$ and 2.0 , respectively. The height of the first cells near the ground and walls is 1.665 mm, yielding the y^+ values at these first cells ranging between 0 and 15, with an average value equal to 5.3. Large y^+ values appear only at the top corners of the windward facades.

Same with the experiments, a uniform wind speed at 1.8 m/s is defined at the inlet of the computational domain. After a sensitivity analysis of turbulence characteristics of the inflow against experimental data of velocity field, a turbulent intensity of 5% and a turbulent length scale of 0.35 m are imposed for the inflow. At the domain outlet, pressure outlet with zero static pressure is specified.

Zero normal velocity and zero normal gradients of all variables are defined at the lateral sides and the top of the domain. The domain ground and the building surfaces are imposed as non-slip walls.

ANSYS Fluent 13.0.0 (Fluent, 2010) is employed to conduct the CFD simulations. A steady-state two-equation RANS model, namely RNG $k-\varepsilon$ model (Yakhot and Orszag, 1986), is used to predict the flow and turbulence fields. RNG $k-\varepsilon$ model is selected due to its good performance in predicting flow in and around buildings (Tominaga and Stathopoulos, 2009; Ai et al., 2013). A two-layer model (Wolfshtein, 1969) and standard wall functions are combined to treat the near-wall regions. SIMPLEC algorithm is used for coupling pressure and momentum equations. The second-order schemes are used to discrete the convection and diffusion terms. Convergence is achieved when all scaled residuals are less than 10^{-5} and the average wind speeds at important locations within the street canyon are stable for over 50 iterations.

Figure 2 shows the velocity component in x direction along some vertical and horizontal lines on the vertical centerplane of the target street canyon. In general, the CFD predictions show a good agreement with the experimental data, with the average relative deviation being less than 20%. It seems that this relative deviation is large. However, most of these velocity magnitudes are around zero, at which the error of anemometers should be in the order of 20%. Some relatively large discrepancies appear at the horizontal lines when $AR = 2.0$. The experimenters (Li et al., 2008a) also reported such levels of discrepancies between experimental data and simulated results. Overall, the CFD method used in this study including the turbulence model selected (namely, RNG $k-\varepsilon$ model) can predict acceptably the flow field in the street canyon, which justifies the use of it in the rest of this paper.

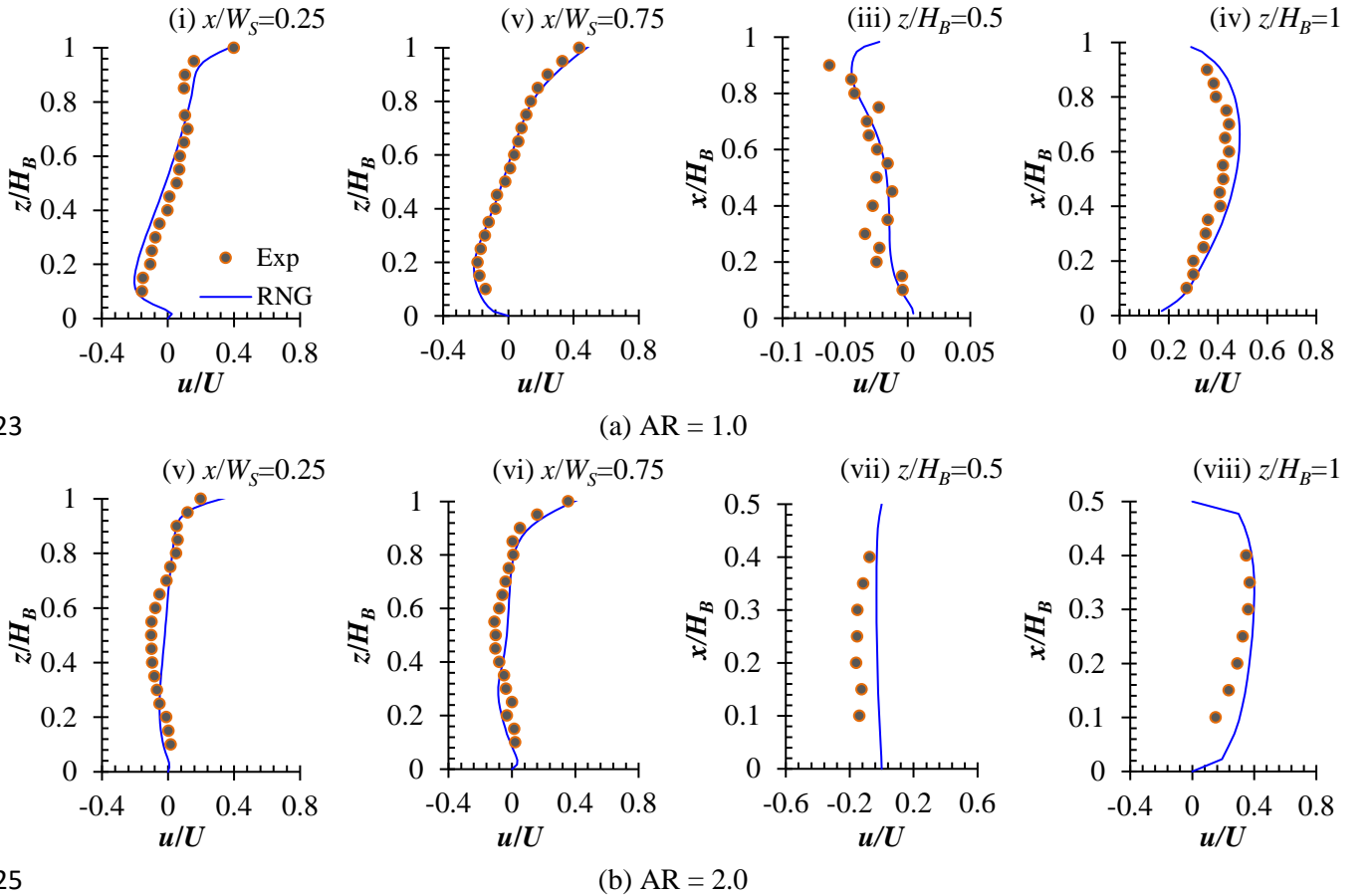


Figure 2 Velocity components in x and z directions along two vertical and two horizontal lines on the vertical centerplane of the target street canyon.

3. CFD simulations: geometry and computational settings

3.1 Computational geometry, domain and grid

A street canyon model formed by two parallel slab-like buildings is investigated in this study (see Figure 3 (a)). Four aspect ratios (H/B), namely 1.0, 2.0, 4.0 and 6.0, are considered, which all belong to the skimming flow regime (Oke, 1987, Ai and Mak, 2015). The height of buildings (H) remains constant, while the width of the street canyon (B) is varied to form different AR values. The street canyon is included into a T-shape computational domain (see Figure 3 (b)). This T-shape computational domain configuration and its dimensions are selected, because many previous studies employed such a T-shape computational domain to investigate the atmospheric flow and related processes in a street canyon (e.g., Kim and Baik, 2001; Liu et al., 2004; Xie et al., 2006; Li et al., 2008b; Kumar et al., 2009; Hu et al., 2009; Moonen et al., 2011; Zhang et al., 2011; Baik et al., 2012; Kwak et al., 2013; Allegrini et al., 2014; Madalozzo et al., 2014), among which there are quite a few (e.g., Liu et al., 2004; Li et al., 2008b; Zhang et al., 2011) used such domain dimensions as shown in Figure 3 (b).

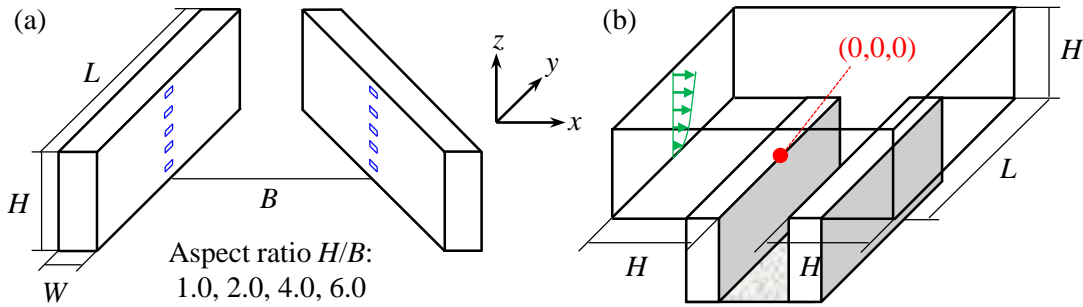
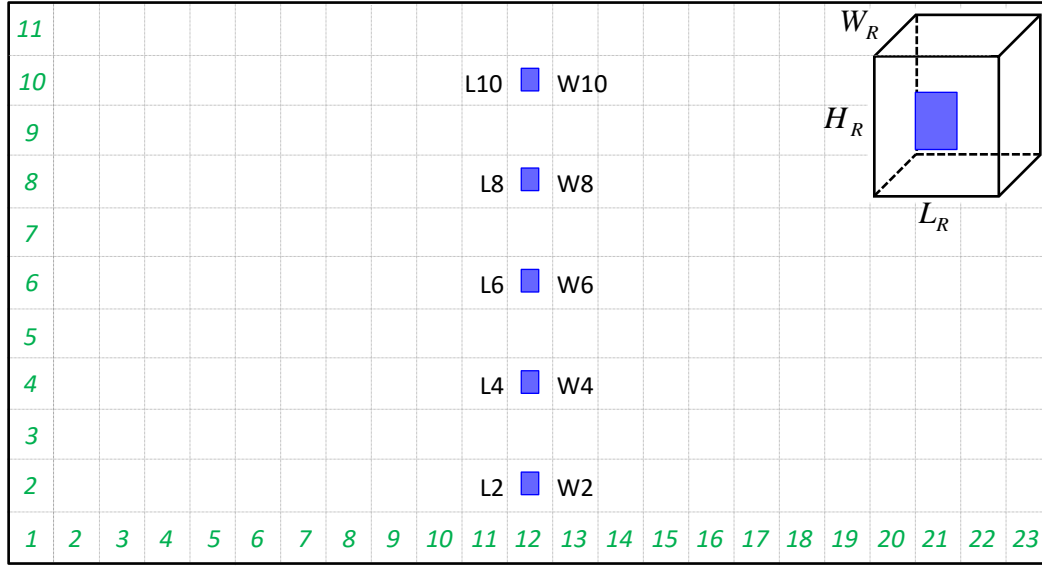


Figure 3 Schematic view of the street canyon model (a) and computational domain (b); note that the two buildings are parallel with each other.

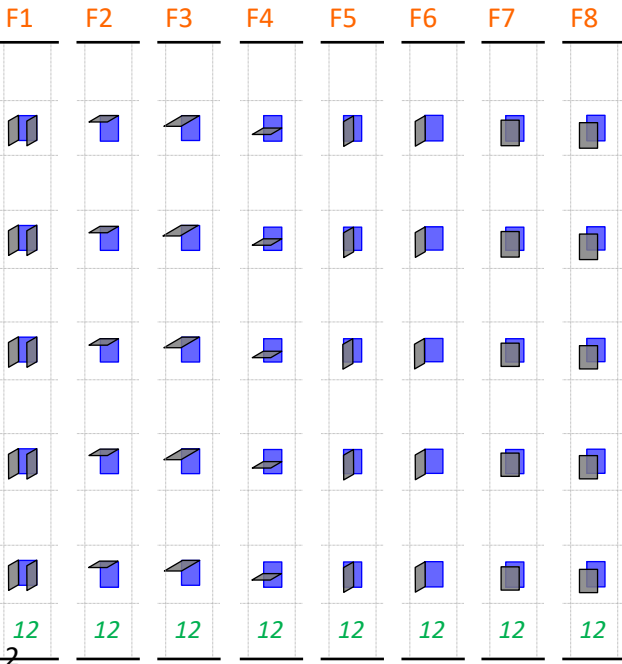
The dimensions of each building are $55.2 \text{ m} \times 29.7 \text{ m} \times 6.2 \text{ m}$ ($L \times H \times W$). Considering that the dimensions of a single room are $2.4 \text{ m} \times 2.7 \text{ m} \times 3.1 \text{ m}$ ($L_R \times H_R \times W_R$), the building models contain 23×11 rooms on both windward and leeward sides (see Figure 4 (a)). The room dimensions are the same with those measured in a real building in Hong Kong (Niu and Tung, 2008; Ai et al., 2013; Ai and Mak, 2016). The selection of the building models is made in compromise between computational cost and the expectation of revealing natural ventilation conditions in buildings near street canyon. In this study, only single-sided natural ventilation is considered, as it is the most common natural ventilation mode in buildings in densely populated urban areas including Hong Kong. Five rooms on the second, fourth, sixth, eighth and tenth floors, respectively, at the horizontal centres of the leeward facade of the upstream building and the windward facade of the downstream building are investigated (see Figure 3 (a) and Figure 4 (a)). Depending on the building facade and floor where a room is located, the rooms are named (see Figure 4 (a)). Apart from this case with flat building facades, eight more cases with protrusive envelope features (F1-F8) are considered to examine their influence on natural ventilation performance in urban buildings (see Figure 4 (b)). The dimensions of the openings and envelope features are shown in Figure 4 (c).

(a) Building facade, room location and name of rooms



1

(b) Envelope features on part of facade



2

(c) Dimensions of opening and envelope features

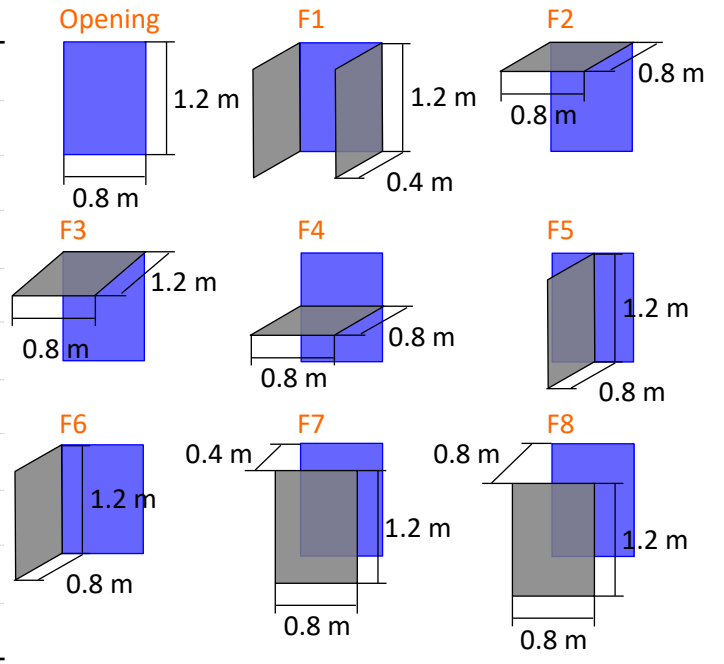


Figure 4 Details of building models of the street canyon, where single-sided naturally ventilated rooms are created along the building center; the ‘L’ and ‘W’ in (a) indicate the leeward facade of the upstream building and windward facade of the downstream building, respectively.

The street canyon is simulated as a 1:15 reduced-scale model, considering that a small model can save computational cost (Ai and Mak, 2014b). With such a reduced-scale model, Reynolds (Re) number independence (Snyder, 1981) must be obeyed. The Re number based on the wind speed and building height in the present study is around 2.4×10^5 , which is sufficiently high to allow an independence of Re number (Snyder, 1981). A high-quality and high-resolution grid near the openings and envelope features is very important for the accurate prediction of the interaction of outdoor flow in the street canyon and indoor flow in the buildings. In this study, hexahedral cells are used to construct the whole computational domain for all cases. A full control over the grid resolution, grid stretching ratio, cell volume skewness and aspect ratios is made. As a result of grid sensitivity test

(as described in Section 3.3), the number of cells used eventually for the baseline cases (namely, without envelope features) are summarized in Table 1. For a certain AR value, the number of cells for cases with envelope features is higher than that for the baseline case. Figure 5 presents the mesh information on a vertical and a horizontal plane across a building of the street canyon. Detailed description of the grid quality is presented in Section 3.3.

Table 1 A summary of the number of cells used for the baseline cases without envelope features.

AR	1.0	2.0	4.0	6.0
No. of cells	6,637,568	5,813,248	4,988,928	4,164,608

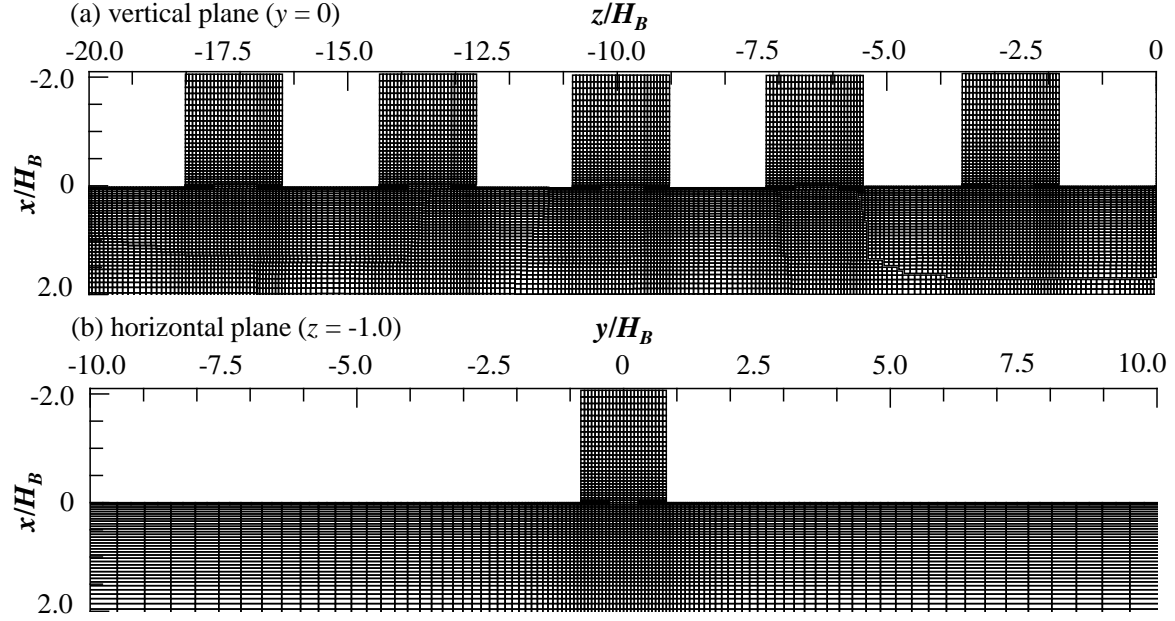


Figure 5 Mesh information on a vertical and a horizontal plane across a building of the street canyon; please see Figure 3 for the location of the planes.

3.2 Boundary conditions and solver settings

The streamwise wind speed profile at the domain inlet is defined using a logarithmic form as shown in Eq. (1), where the von Karman constant $\kappa = 0.4187$ and the aerodynamic roughness height $z_0 = 0.001$ m. Such a roughness height corresponds to a flat terrain (Wieringa, 1992) and thus a thin boundary layer, which is selected for building tops essentially because of two reasons. First, the building top is assumed to be relatively flat, which should have a very small roughness height compared to the general roughness height on the urban ground, where buildings, trees and other constructions represent roughness. Second, a small roughness height allows a fine near-wall mesh density, which is important for accurately predicting the near-wall flow field. In this study, the reference velocity (U_{ref}) at the height of $z_{ref} = 2H$ are $U_{ref} = 4.2$ m/s and $z_{ref} = 59.4$ m. Note that this reference velocity is derived from Eq. (1) based on the yearly averaged mean wind speed at the height of 10 m (U_{10}) recorded at Hong Kong observatory, which is located in a roughly open country with $z_0 = 0.1$ m, according to the roughness classification by Wieringa (1992). Based on the values of κ , z_0 , U_{ref} and z_{ref} , the friction velocity of atmospheric flow above the building tops (u^*) can be obtained from Eq. (1), which is 0.17 m/s. The turbulent kinetic energy k is calculated from the mean wind speed profile U in Eq. (1) and the streamwise turbulence intensity I_u using the correlation,

$k(z) = 1.5 \cdot (I_u(z) \cdot U(z))^2$, which is finally fitted into Eq. (2) to ensure homogeneity along computational domain (Ai and Mak, 2013). The streamwise turbulence intensity I_u is defined as 15% above the building top, which is similar with that above a ground with such a roughness condition. Eventually, the model coefficients in Eqs (2) and (3) are $M_1 = 0.0344$ and $M_2 = 0.23747$. The empirical constant C_μ is determined by Eq. (4) and the turbulence dissipation Prandtl number σ_ε by Eq. (5) (Ai and Mak, 2013). The term z_p in Eq. (4) represents the distance between the geometrical center of the first cells and their nearest walls. On the domain ground and building facades, the two-layer model with roughness modifications is used (Wolfshtein, 1969; Ai and Mak, 2013). The geometrical roughness height on the domain ground is $K_S = 0.01$ m, according to the relation of $K_S = 9.793z_0/C_S$ and $C_S = 0.9793$ (Blocken et al., 2007).

The boundary conditions for domain outlet, lateral sides and top as well as for building surfaces are identical to those used in the validation study. In addition, the solver settings are the same with those used in the validation study. In order to examine the achievement of horizontal homogeneity, or the extent of unintended streamwise gradients, CFD simulation in an empty computational domain is performed using the above described computational settings. Figure 6 presents the vertical profiles of U , k and ε at both the inlet and the location of interest (where the street canyon is located), which indicates that the horizontal homogeneity for both velocity and turbulent profiles is generally achieved along the computational domain.

$$U = \frac{u^*}{\kappa} \ln \left(\frac{z + z_0}{z_0} \right) \quad (1)$$

$$k = \sqrt{M_1 \cdot \ln(z + z_0) + M_2} \quad (2)$$

$$\varepsilon = \frac{u^* \sqrt{C_\mu}}{\kappa(z + z_0)} \sqrt{M_1 \cdot \ln(z + z_0) + M_2} \quad (3)$$

$$C_\mu = \frac{u^{*4}}{\sqrt{M_1 \cdot \ln(z_p + z_0) + M_2}} \quad (4)$$

$$\sigma_\varepsilon = \frac{\kappa^2 (k^2 - M_1 / 2)}{u^{*2} (M_2 - M_1) k} \quad (5)$$

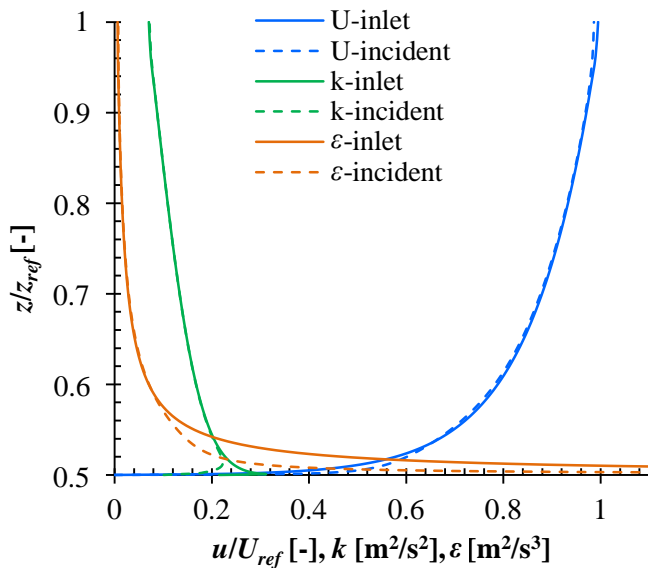


Figure 6 Horizontal homogeneity analysis: comparison of inlet and incident profiles in the atmospheric boundary layer of an empty domain.

3.3 Grid sensitivity test

Grid sensitivity test is performed for the baseline street configuration of $AR = 1.0$ to ensure the independence of numerical solutions from the cell number. Three grids, namely a coarse grid, a basic grid and a fine grid are constructed, where the latter two grids are obtained by refining the coarse grid with a factor of approximately 1.2. Detailed information of the three grids is summarized in Table 2. In general, all of the three grids are high-resolution ($y^+ < 30.0$), with the near-wall boundary layer being meshed and thus resolved. Numerical solutions predicted by the three grids are compared. Figure 7 presents the ACH values of the rooms given by the three grids. Note that the calculation method of the ACH value is described by Eq. (6) at the beginning of Section 4. It shows that the results predicted by the basic grid are very close to those predicted by the fine grid, with a mean deviation of 4.0%, whereas such a deviation is 17.9% between the coarse and basic grids. This comparison suggests that the basic grid is sufficiently fine to obtain accurate results, which is thus used in this study. The grid arrangement, particularly the resolution and stretching ratio, for other street configurations of $AR = 2.0, 4.0$ and 6.0 is the same with this for the case of $AR = 1.0$.

Table 2 A summary of the three grids used for grid sensitivity test.

Grid type	No. of cells	Minimum length (m)	Minimum volume (m^3)	Mean y^+ on building facades and their ranges
Fine	11,914,840	1.7×10^{-3}	9.7×10^{-9}	3.8 (0; 9.0]
Basic	6,637,568	2.0×10^{-3}	1.9×10^{-8}	4.5 (0; 10.5]
Coarse	3,847,608	5.7×10^{-3}	2.4×10^{-7}	11.0 (0; 24.0]

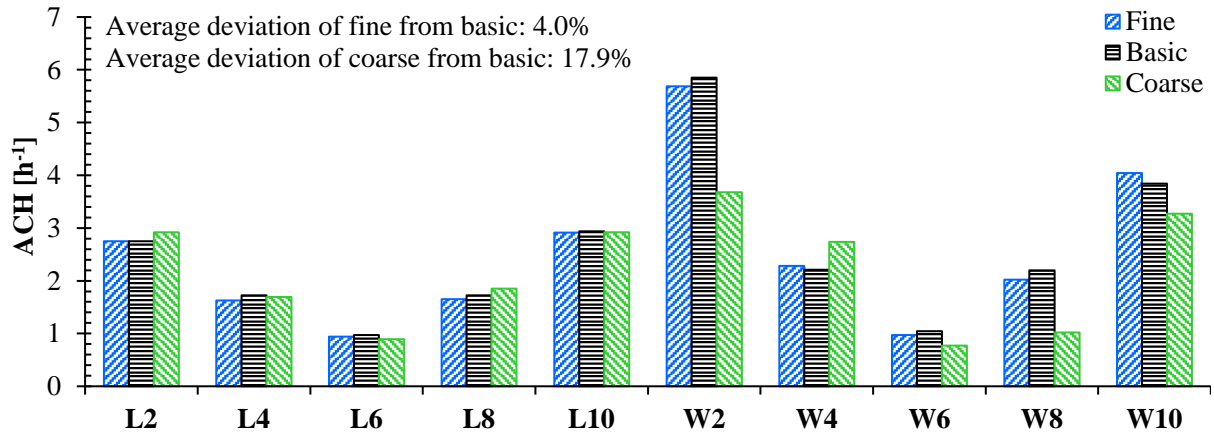


Figure 7 Grid sensitivity test: comparison of mean ACH values of the ten rooms predicted using the three types of grids.

4. CFD simulations: results and analysis

The ventilation rate is almost the most important parameter used to evaluate natural ventilation performance of buildings. Calculation of the single-sided ventilation rate can be made based on either mean-velocity-based integral method or concentration-based tracer gas method (Jiang et al., 2003; Ai and Mak, 2014a). This study employs the integral method, which integrates the mean velocities on an opening that are extracted from a time-averaged flow field generated by the steady RANS simulations:

$$Q_{mean} = \frac{1}{2} \sum_{m=1}^M \sum_{n=1}^N |U_{m,n}| \Delta y_m \Delta z_n \quad (6)$$

where Q_{mean} is mean ventilation rate, $U_{m,n}$ mean velocity at a cell (m, n), and Δy_m and Δz_n dimensions of the cell. The ACH value can be then obtained by: $ACH = Q_{mean}/V_{room}$, in which V_{room} is the volume of a room.

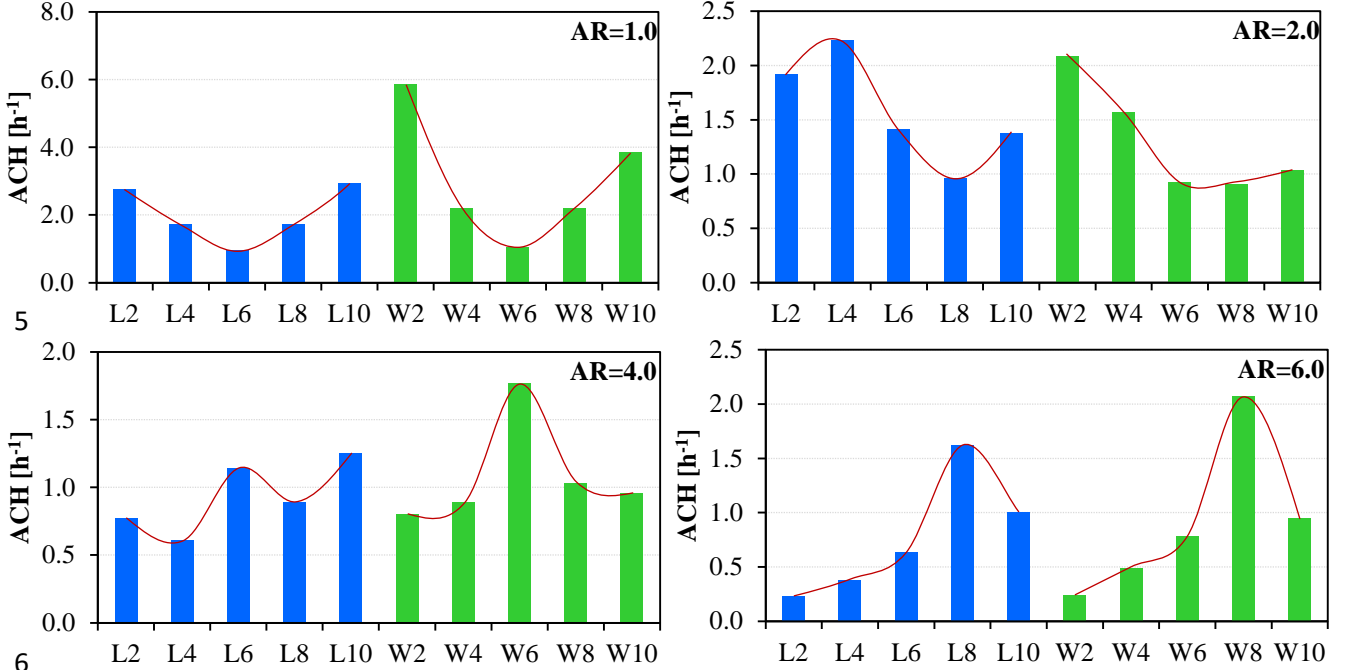


Figure 8 ACH values of rooms in buildings near the street canyon under different aspect ratios.

4.1 Influence of aspect ratio (no feature)

Figure 8 presents the ACH values of rooms at both leeward and windward sides of the street canyon under different aspect ratios. It is obvious that the ACH values along height are not uniformly distributed. For $AR = 1.0$, the rooms located on the lowest floor and the top most floor show the best ventilation performance. This distribution of ACH values is similar with that observed on an isolated building (Ai et al., 2013). The locations of the rooms that have the best ventilation performance shift with the increase of aspect ratio. The reason for the distributions of ACH values along height can be obtained from the analysis of the flow patterns inside street canyons (see Figure 9).

For $AR = 1.0$, a large and strong vortex is formed inside the street canyon. Rooms located at the lower and top parts of the street canyon would have the highest possibility to experience normal-to-facade near-wall flows, which contribute mostly to the indoor and outdoor flow exchange. Figure 10 presents the contours of normal-to-facade velocity component at the openings of the windward rooms, which indicates that there are stronger inflows and outflows on the openings located at the lower and top parts of the street canyon than those at the middle part. This phenomenon is consistent with the distribution of ACH values (see Figure 8: $AR = 1.0$). Although it is a fact that along-facade flows still contribute to indoor ventilation due to their turbulent effects (Ai and Mak, 2014a), for the case with perpendicular wind direction studied in this paper, the normal-to-facade flows should be the main contributor of the indoor ventilation. When $AR = 2.0$, two vortices are formed and they interact at the lower part of the street canyon, which produces opportunities for nearby rooms to have higher ventilation rates (see Figure 8: $AR = 2.0$). Similar reasons can be found for the cases of $AR = 4.0$ and $AR = 6.0$. However, when $AR = 6.0$, the skimming flow above the street canyon cannot penetrate deeply into the lower part of the street canyon, which results in the very low ventilation rates for the rooms located at the lower part of the street canyon. These distributions of ACH values along height under different

aspect ratios are important findings, which reveal the locations where the best and the worst ventilation could occur.

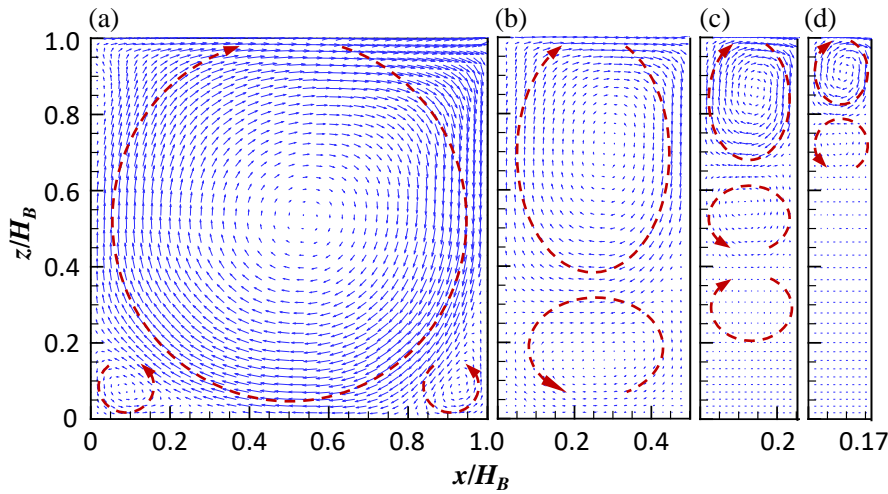


Figure 9 Flow vectors on the vertical centerplane of the street canyon under different aspect ratios: (a) AR = 1.0, (b) AR = 2.0, (c) AR = 4.0 and (d) AR = 6.0.

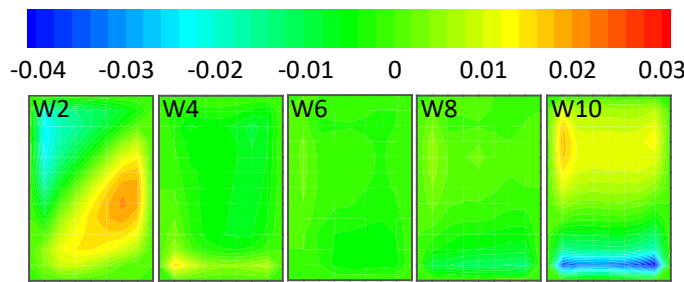


Figure 10 Nondimensional velocity component (u/U) along x direction (normal-to-facade direction) on windward openings for AR = 1.0.

Figure 11 shows the average ACH values of rooms for different aspect ratios. ACH values on both the leeward and windward sides decrease with the increase of aspect ratio. Taking the case of AR = 1.0 as the base case, the percentage decreases of ACH of other cases with a higher AR are calculated. In general, a large decrease of ACH is observed when the aspect ratio is increased. However, such a decrease becomes slow gradually. Obviously, it is more difficult for the atmospheric flow above a street canyon to penetrate deeply into the inside of a deeper street canyon (namely, with a higher aspect ratio). Previous studies regarding urban physics show that wind speed in urban areas is seriously decreased due to the increased roughness caused by complex constructions when compared to that in rural areas (Ai and Mak, 2015; Oke, 1987; HKPD, 2005; Georgakis and Santamouris, 2006). Decreased wind speeds in a deep street canyon would result in lowered pressure differences to drive indoor natural ventilation. Therefore, natural ventilation performance in urban buildings, especially in dense areas, drops largely compared to rural areas (Georgakis and Santamouris, 2006; Qian et al., 2010; van Hooff and Blocken, 2010; Gao and Lee, 2012). The findings in this section suggest that on one hand describing the major surroundings in detail is important when assessing natural ventilation performance in buildings and on the other hand the aspect ratio of a street canyon is an important factor influencing the building natural ventilation.

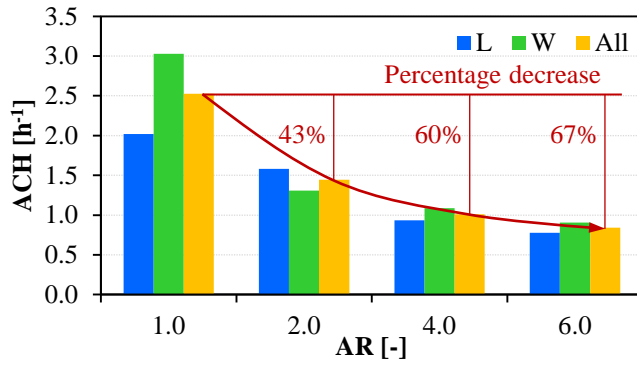


Figure 11 Average ACH values of all rooms at leeward facade (L), windward facade (W) and both facades (All), where the percentage decreases of ACH in comparison to the case of AR = 1.0 are also presented.

4.2 Influence of envelope features

Figure 12 shows the average ACH values of rooms at leeward facade, windward facade and both facades for the street canyon of AR = 1.0. In general, the average ACH value of all rooms shows a similar trend with those of either leeward or windward rooms. Therefore, the average ACH value of all rooms is used as the parameter to analyse the performance of each envelope feature in improving natural ventilation performance of buildings.

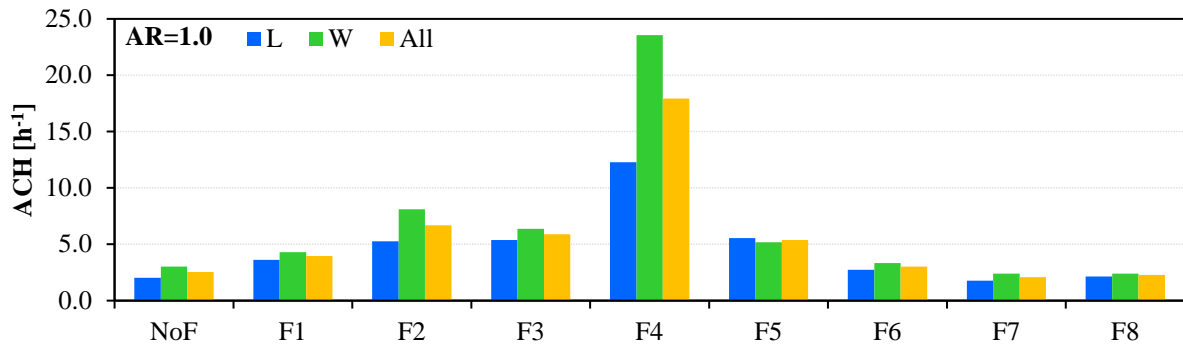


Figure 12 Average ACH values of rooms at leeward facade (L), windward facade (W) and both facades (All) for the street canyon of AR = 1.0, where NoF represents ‘no feature’.

Figure 13 presents quantitatively the influence of the presence of a certain envelope feature on the average ACH value. For all aspect ratios, the presence of envelope features F1-F6 improve natural ventilation performance of buildings, while features F7-F8 degrade it except for the F8 of AR = 4.0. For AR = 1.0, F4 shows the best performance among all eight envelope features in terms of the percentage increase of average ACH value, which is followed by F2, F3, F5, F1 and F6. This ranking sequence remains the same for AR = 2.0, which, however, is changed slightly when AR = 4.0 and significantly when AR = 6.0. Based on AR = 1.0, the following paragraphs first analyse why a certain envelope feature can improve or degrade the indoor ventilation performance, and then explain why the ranking sequence changes when AR becomes 6.0.

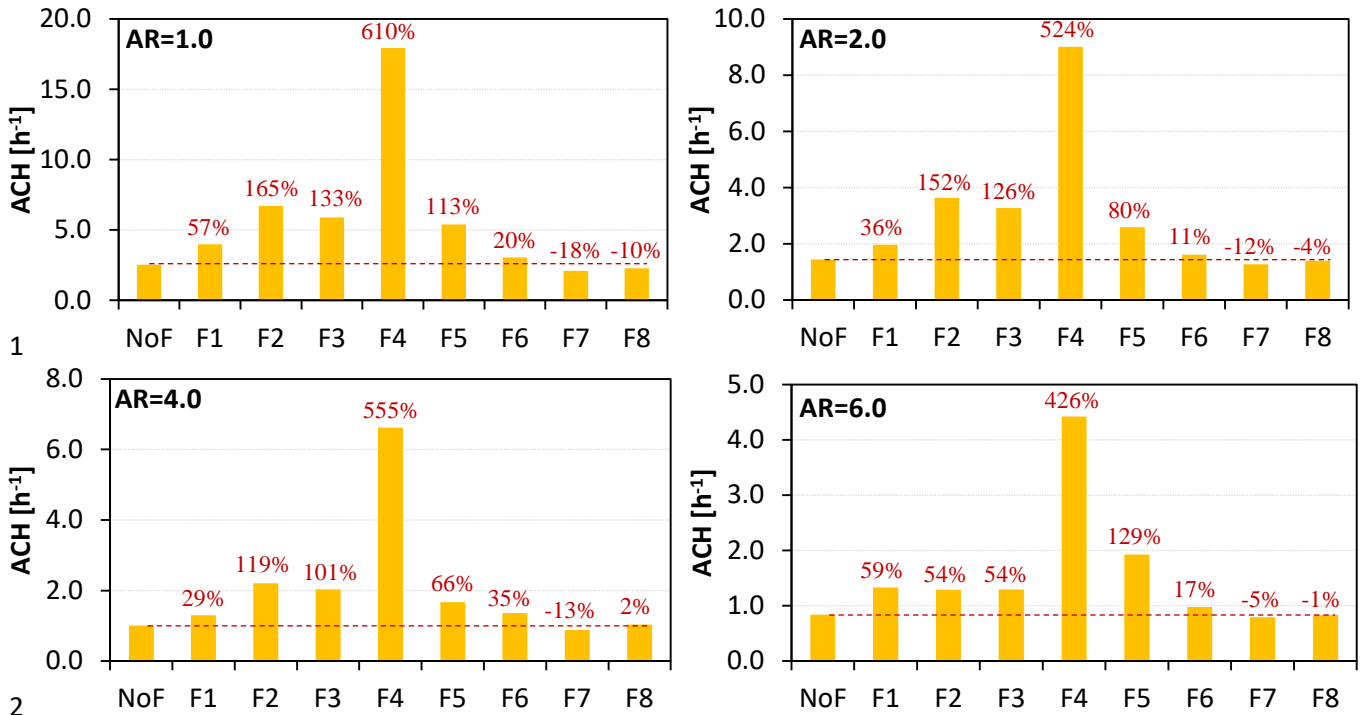


Figure 13 Average ACH values of all rooms at both the leeward and windward facades of the street canyon under different aspect ratios, where the percentage increases of ACH in comparison to the case of NoF are also presented.

The distribution and magnitude of the normal-to-facade velocity component at an opening are important parameters indicating the indoor ventilation performance. Figure 14 presents the contour of nondimensional velocity component (u/U) along x direction (normal-to-facade direction) on the opening of W8 for $AR = 1.0$. Here the W8 is just taken as a representative room to make analysis, which is intended to reveal the general influence of envelope features on natural ventilation performance.

For F4 (see both Figure 14 and Figure 4 (c)), the presence of a horizontal feature at the middle of the opening breaks the downward or upward flows and thus creates a large pressure difference between the upper and lower parts of the opening, which helps effectively to drive indoor natural ventilation. Similar flow patterns around an envelope feature are observed in our previous studies on balcony aerodynamics (Ai et al., 2013; Ai and Mak, 2016).

For F2 and F3, the presence of a horizontal feature at the top of the opening can also break the downward or upward flows and creates a pressure difference between the regions above and underneath the feature. However, different from F4, such a pressure difference cannot serve entirely to drive natural ventilation. In comparison, a shorter horizontal feature (F2) shows a better performance than a longer one (F3). The reason should be that the blockage effect of the feature to flow becomes gradually dominated when the length of the horizontal feature increases.

For F5, F1 and F6, the presence of vertical feature(s) function to enhance and utilize the imbalance of flows between the two sides of the feature, especially when the flow patterns at the two sides are not symmetrical. Their presence increases the turbulence and creates a pressure difference at the opening, which results in obvious inflow and outflow at the two sides of the feature. Similar to horizontal feature, a vertical feature located at the middle, instead of end, of an opening is better for improving natural ventilation performance. It is interesting to note that the presence of two vertical features (F1) shows even better performance than the presence of one vertical feature at one side of the opening (F6). This should be attributed to that the presence of two features enhances the pressure

difference at the opening when compared to the presence of one feature at one side of the opening (see Figure 14).

For F7 and F8, the presence of a horizontal feature in front of an opening forms as a curtain to decrease the flow movement along the normal-to-facade direction and to stabilize the near-opening flows, which all help negatively to improve natural ventilation performance of buildings. Therefore, the F7 and F8 should always be avoided in building design at least from the ventilation point of view.

For $AR = 6.0$, the F5, instead of F2, ranks number 2 among the eight envelope features. This is originally because the flow movement inside the deep street canyon of $AR = 6.0$ is very weak when compared to other street canyons of $AR = 1.0, 2.0$ and 4.0 . Within a flow field with a relatively strong along-facade downward or upward flow ($AR = 1.0, 2.0$ and 4.0), the presence of a horizontal feature at the top of the opening (F2) performs well in creating pressure difference and thus driving indoor/outdoor flow exchange. Such a capability of a horizontal feature is, however, lowered significantly within a weak-movement flow field ($AR = 6.0$).

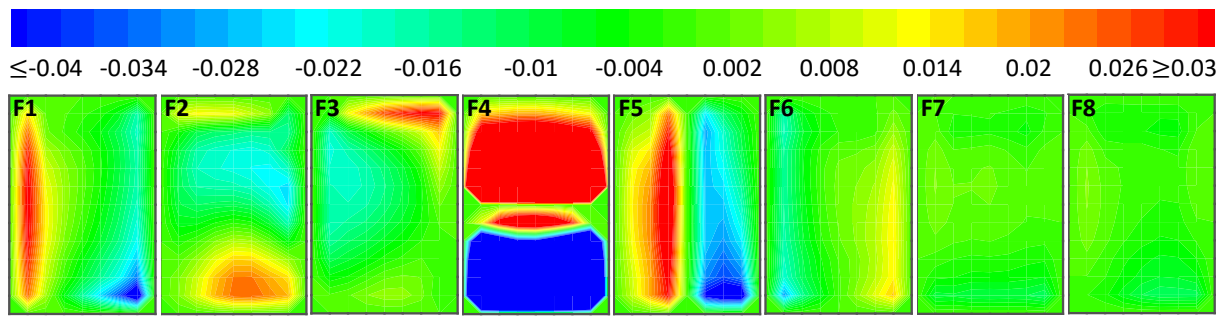


Figure 14 Contour of nondimensional velocity component u/U along x direction (normal-to-facade direction) on opening W8 for $AR = 1.0$.

5. Discussion

This paper investigates the natural ventilation performance of buildings in an urban context from both street configuration and envelope design perspectives. Four aspect ratios of a street canyon and eight envelope features are investigated. The findings should provide important information for increasing the understanding of natural ventilation in urban buildings and its influencing factors. However, the authors have to reveal the following limitations of the study presented in this paper.

First, this study investigates only the perpendicular wind direction, as it is the most widely investigated wind direction due to its association with the worst condition for ventilation and pollutant dilution of a street canyon (Ai and Mak, 2015). However, it is expected that the influence of street canyon aspect ratio and envelope feature on natural ventilation performance of buildings may change with wind direction. In order to have a more complete observation of natural ventilation performance in urban buildings and its influencing factors, it is necessary to investigate other wind directions. In particular, a vertical feature at the middle of an opening may perform very well in enhancing indoor/outdoor flow exchange when the prevailing wind direction is parallel to the street canyon.

Second, this study is limited to purely wind-driven conditions. Although wind effect is the dominated driving force in urban environments under most periods of time, buoyancy effect due to temperature differences should not be ignored in some circumstances, especially when the wind is relatively weak. Some previous studies (Ai and Mak, 2015) show that, in street canyons under a certain weather condition, the temperature difference between surfaces with and without direct solar radiation could reach up to $19\text{ }^{\circ}\text{C}$ (Santamouris et al., 1999). Therefore, it is necessary to investigate the combined effect of wind and buoyancy effects.

Third, this study uses the steady-state RANS turbulence model to predict the flow field and use the mean-velocity-based integral method to calculate the ventilation rates. Both the turbulence model and the integral method have their inherent drawbacks and would thus inevitably result in inaccurate calculations. Fortunately, this study focuses on evaluating the relative influence of aspect ratio and envelope feature, which is based on the comparison with a base case. It is believed that such a relative evaluation would counteract largely the inaccuracy caused by the selected RANS model and integral method. However, in order to obtain more accurate flow field and ventilation rates, large eddy simulation (LES) and concentration-based method (Ai and Mak, 2014a) are excellent alternative options, respectively.

6. Conclusions

Previous studies regarding natural ventilation in buildings are mostly limited to isolated buildings. This study investigates natural ventilation performance of buildings in an urban context under a perpendicularly incident wind. Four aspect ratios are considered to evaluate the influence of street configuration, while eight envelope features are examined to explore the appropriate envelope design that can increase the adaptability of buildings to dense urban environments.

Since the atmospheric flow above a street canyon is more difficult to penetrate deeply into a deeper street canyon, ventilation performance of buildings is decreased with the increase of aspect ratio of a street canyon. Compared to the case of $AR = 1.0$, the percentage decrease of ACH values are, on average, 43%, 60% and 67% for the cases of $AR = 2.0$, 4.0 and 6.0, respectively. Influenced by flow pattern inside a street canyon, ACH values of rooms along height of a building are not uniformly distributed. Such a distribution varies significantly with the change of aspect ratio. These findings (namely, ACH values and their distributions) suggest that aspect ratio is an important parameter that should be considered when designing natural ventilation of urban buildings.

Envelope design is a good strategy for improving the adaptability of buildings to dense urban environments. A horizontal feature at the middle of an opening (F4 in this study) presents the best performance in improving the indoor natural ventilation performance. This implies that an appropriate envelope feature is one that can effectively break the along-facade flow and utilize the impinging flow momentum to create a large pressure difference between different locations of an opening. Conversely, a vertical feature in front of an opening is inappropriate, as it decelerates the normal-to-facade flows and stabilizes the near-opening flows.

Acknowledgement

The work described in this paper was financially supported by a grant from the Environment and Conservation Fund of Hong Kong (Project ECF 18/2014). The first author, Dr. Zhengtao Ai, at the time of submitting this paper, was a H.C. Ørsted-COFUND postdoctoral researcher, who was supported by a funding from the People Programme (Marie Curie Actions) of the European Union's Seventh Framework Programme (FP7/2007-2013) under REA grant agreement no. 609405 (COFUNDPostdocDTU).

References

- Ai, Z.T., Mak, C.M., 2013. CFD simulation of flow and dispersion around an isolated building: effect of inhomogeneous ABL and near-wall treatment. *Atmos. Environ.* 77, 568-578.
- Ai, Z.T., Mak, C.M., Niu, J.L., 2013. Numerical investigation of wind-induced airflow and interunit dispersion characteristics in multistory residential buildings. *Indoor Air* 23, 417-429.
- Ai, Z.T., Mak, C.M., 2014a. Modeling of coupled urban wind flow and indoor air flow on a high-density near-wall mesh: sensitivity analyses and case study for single-sided ventilation. *Environ. Model. Softw.* 60, 57-68.

- 1 Ai, Z.T., Mak, C.M., 2014b. Potential use of reduced-scale models in CFD simulations to save
2 numerical resources: Theoretical analysis and case study of flow around an isolated building. *J.*
3 *Wind Eng. Ind. Aerodyn.* 134, 25-29.
- 4 Ai, Z.T., Mak, C.M., 2015. From street canyon microclimate to indoor environmental quality in
5 naturally ventilated urban buildings: Issues and possibilities for improvement. *Build. Environ.* 94,
6 489-503.
- 7 Ai, Z.T., Mak, C.M., 2016. Large eddy simulation of wind-induced interunit dispersion around
8 multistory buildings. *Indoor Air* 26, 259-273.
- 9 Allegrini, J., Dorer, V., Carmeliet, J., 2014. Buoyant flows in street canyons: Validation of CFD
10 simulations with wind tunnel measurements. *Build. Environ.* 72, 63-74.
- 11 Andreou, E., Axarli, K., 2012. Investigation of urban canyon microclimate in traditional and
12 contemporary environment: Experimental investigation and parametric analysis. *Renew. Energ.* 43,
13 354-363.
- 14 Baik, J.J., Kwak, K.H., Park, S.B., Ryu, Y.H., 2012. Effects of building roof greening on air quality in
15 street canyons. *Atmos. Environ.* 61, 48-55.
- 16 Blocken, B., Gualtieri, C., 2012. Ten iterative steps for model development and evaluation applied to
17 Computational Fluid Dynamics for Environmental Fluid Mechanics. *Environ. Modell. Softw.* 33,
18 1-22.
- 19 Blocken, B., Stathopoulos, T., Carmeliet, J., 2007. CFD simulation of the atmospheric boundary layer:
20 wall function problems. *Atmos. Environ.* 41, 238-252.
- 21 Buller, P.S.J., 1976. Wind speeds measured within an urban area. Report No. 2, Building
22 Establishment Note N12/76, DoE, Building Research Station, Watford, UK.
- 23 Caciolo, M., Stabat, P., Marchio, D., 2011. Full scale experimental study of single-sided ventilation:
24 Analysis of stack and wind effects. *Energ. Buildings* 43, 1765-1773.
- 25 Caciolo, M., Stabat, P., Marchio, D., 2012. Numerical simulation of single-sided ventilation using
26 RANS and LES and comparison with full-scale experiments. *Build. Environ.* 50, 202-213.
- 27 Dascalaki, E., Santamouris, M., Argiriou, A., Helmis, C., Asimakopoulos, D.N., Papadopoulos, K.,
28 Soilemes, A., 1996. On the combination of air velocity and flow measurements in single sided
29 natural ventilation configurations. *Energ. Buildings* 24, 155-165.
- 30 Fluent, 2010. ANSYS FLUENT 13.0 Theory Guide. Turbuelnce, Canonsburg, PA, ANSYS Inc.
- 31 Franke, J., Hellsten, A., Schlunzen, H., Carissimo, B., 2007. Best practice guideline for the CFD
32 simulation of flows in the urban environment – COST Action 732. COST office.
- 33 Gao, C.F., Lee, W.L., 2012. The influence of surrounding buildings on the natural ventilation
34 performance of residential dwellings in Hong Kong. *Int. J. Vent.* 11(3), 297-310.
- 35 Georgakis, C., Santamouris, M., 2006. Experimental investigation of air flow and temperature
36 distribution in deep urban canyons for natural ventilation purposes. *Energ. Buildings* 38, 367-376.
- 37 Gilkeson, C.A., Camargo-Valero, M.A., Pickin, L.E., Noakes, C.J., 2013. Measurement of ventilation
38 and airborne infection risk in large naturally ventilated hospital wards. *Build. Environ.* 65, 35-48.
- 39 Haghighat, F., Brohus, H., Rao, J., 2000. Modelling air infiltration due to wind fluctuations – a review.
40 *Build. Environ.* 35, 377-385.
- 41 Haghighat, F., Rao, J., Fazio, P., 1991. The influence of turbulent wind on air change rates – a
42 modelling approach. *Build. Environ.* 26(2), 95-109.
- 43 HKPD, 2005. Feasibility study for establishment of air ventilation assessment system, final report, the
44 government of the Hong Kong special administrative region. Hong Kong Planning Department;
45 2005. http://www.pland.gov.hk/pland_en/p_study/comp_s/avas/papers%26reports/final_report.pdf.
46 page 96.
- 47 Hu, L.H., Huo, R., Yang, D., 2009. Large eddy simulation of fire-induced buoyancy driven plume
48 dispersion in an urban street canyon under perpendicular wind flow. *J Hazard. Mater.* 166, 394-406.

- 1 Jiang, Y., Alexander, D., Jenkins, H., Arthur, R., Chen, Q., 2003. Natural ventilation in buildings:
2 measurement in a wind tunnel and numerical simulation with large-eddy simulation. *J. Wind Eng.*
3 *Ind. Aerodyn.* 91, 331-353.
- 4 Jiang, Y., Chen, Q., 2001. Study of natural ventilation in buildings by large eddy simulation. *J. Wind*
5 *Eng. Ind. Aerodyn.* 89, 1155-1178.
- 6 Karava, P., Stathopoulos, T., Athienitis, A.K., 2011. Airflow assessment in cross-ventilated buildings
7 with operable facade elements. *Build. Environ.* 46, 266-279.
- 8 Kim, J.J., Baik, J.J., 2001. Urban street-canyon flows with bottom heating. *Atmos. Environ.* 35, 3395-
9 3404.
- 10 Kitous, S., Bensalem, R., Adolphe, L., 2012. Airflow patterns within a complex urban topography
11 under hot and dry climate in the Algerian Sahara. *Build. Environ.* 56, 162-175.
- 12 Kumar, P., Garmory, A., Ketzel, M., Berkowicz, R., Britter, R., 2009. Comparative study of measured
13 and modelled number concentrations of nanoparticles in an urban street canyon. *Atmos. Environ.*
14 43, 949-958.
- 15 Kwak, K.H., Baik, J.J., Lee, K.Y., 2013. Dispersion and photochemical evolution of reactive
16 pollutants in street canyons. *Atmos. Environ.* 70, 98-107.
- 17 Larsen, T.S., Heiselberg, P., 2008. Single-sided natural ventilation driven by wind pressure and
18 temperature difference. *Energ. Buildings* 40, 1031-1040.
- 19 Li, H., Li, X., Qi, M., 2014. Field testing of natural ventilation in college student dormitories (Beijing,
20 China). *Build. Environ.* 78, 36-43.
- 21 Linden, P.F., 1999. The fluid mechanics of natural ventilation. *Annu. Rev. Fluid Mech.* 31, 201-238.
- 22 Liu, C.H., Barth, M.C., Leung, D.Y.C., 2004. Large-eddy simulation of flow and pollutant transport in
23 street canyons of different building-height-to-street-width ratios. *J. Appl. Meteor.* 43, 1410-1424.
- 24 Li, X.X., Leung, D.Y.C., Liu, C.H., 2008a. Physical modelling of flow field inside urban street
25 canyons. *J. Appl. Meteorol. Clim.* 47, 2058-2067.
- 26 Li, X.X., Liu, C.H., Leung, D.Y.C., 2008b. Large-eddy simulation of flow and pollutant dispersion in
27 high-aspect-ratio urban street canyons with wall model. *Bound.-Layer Meteor.* 129, 249-268.
- 28 Li, X.X., Liu, C.H., Leung, D.Y.C., Lam, K.M., 2006. Recent progress in CFD modelling of wind
29 field and pollutant transport in street canyons. *Atmos. Environ.* 40, 5640-5658.
- 30 Madalozzo, D.M.S., Braun, A.L., Awruch, A.M., Morsch, I.B., 2014. Numerical simulation of
31 pollutant dispersion in street canyons: Geometric and thermal effects. *Appl. Math. Model.* 38,
32 5883-5909.
- 33 Manning, A.J., Nicholson, K.J., Middleton, D.R., Rafferty, S.C., 2000. Field study of wind and traffic
34 to test a street canyon pollution model. *Environ. Monit. Assess.* 60, 283-313.
- 35 Moonen, P., Dorer, V., Carmeliet, J., 2011. Evaluation of the ventilation potential of courtyards and
36 urban street canyons using RANS and LES. *J. Wind Eng. Ind. Aerodyn.* 99, 414-423.
- 37 Nakamura, Y., Oke, T.R., 1988. Wind, temperature and stability conditions in an east-west oriented
38 urban canyon. *Atmos. Environ.* 22(12), 2691-700.
- 39 Niachou, K., Livada, I., Santamouris, M., 2008. Experimental study of temperature and airflow
40 distribution inside an urban street canyon during hot summer weather conditions – Part 2: Airflow
41 analysis. *Build. Environ.* 43, 1393-1403.
- 42 Niu, J.L., Tung, T.C.W., 2008. On-site quantification of re-entry ratio of ventilation exhausts in multi-
43 family residential buildings and implications. *Indoor Air* 18, 12-26.
- 44 Oke, T.R., 1987. *Boundary layer climates*. 2nd ed. New York: Routledge.
- 45 Phaff, H., De Gids, W., 1982. Ventilation rates and energy consumption due to open windows: A brief
46 overview of research in the Netherlands. *Air Infiltration Review* 4(1), 4-5.
- 47 Qian, H., Li, Y., Seto, W.H., Ching, P., Chiang, W.H., Sun, H.Q., 2010. Natural ventilation for
48 reducing airborne infection in hospitals. *Build. Environ.* 45, 559-565.

- 1 Santamouris, M., Papanikolaou, N., Koronakis, I., Livada, I., Asimakopoulos, D., 1999. Thermal and
2 air flow characteristics in a deep pedestrian canyon under hot weather conditions. *Atmos. Environ.*
3 33, 4503-4521.
- 4 Santamouris, M., Synnefa, A., Assimakopoulos, M., Livada, I., Pavlou, K., Papaglastra, M., et al.,
5 2008. Experimental investigation of the air flow and indoor carbon dioxide concentration in
6 classrooms with intermittent natural ventilation. *Energ. Buildings* 40, 1833-1843.
- 7 Snyder, W.H., 1981. Guideline for Fluid Modeling of Atmospheric Diffusion, Meteorology and
8 Assessment. Division Environmental Sciences Research Laboratory. U.S. Environmental
9 Protection Agency, Research Triangle Park, NC.
- 10 Straw, M.P., 2000. Computation and measurement of wind induced ventilation. Thesis, University of
11 Nottingham.
- 12 Tominaga, Y., Mochida, A., Yoshie, R., Kataoka, H., Nozu, T., Yoshikawa, M., Shirawasa, T., 2008.
13 AIJ guidelines for practical applications of CFD to pedestrian wind environment around buildings.
14 *J. Wind Eng. Ind. Aerodyn.* 96(10-11), 1749-1761.
- 15 Tominaga, Y., Stathopoulos, T., 2009. Numerical simulation of dispersion around an isolated cubic
16 building: comparison of various types of $k-\epsilon$ models. *Atmos. Environ.* 43, 3200-3210.
- 17 Wang, H., Chen, Q., 2012. A new empirical model for predicting single-sided, wind-driven natural
18 ventilation in buildings. *Energ. Buildings* 54, 386-394.
- 19 Warren, P., 1977. Ventilation through openings on one wall only. Proceedings of International Centre
20 for Heat and Mass Transfer Seminar "Energy Conservation in Heating, Cooling, and Ventilating
21 Buildings", Washington, 189-209.
- 22 Wieringa, J., 1992. Updating the Davenport roughness classification. *J. Wind Eng. Ind. Aerodyn.* 41,
23 357-368.
- 24 Wolfshtein, M., 1969. The velocity and temperature distribution of one-dimensional flow with
25 turbulence augmentation and pressure gradient. *Int. J. Heat Mass Transf.* 12, 301-318.
- 26 van Hooff, T., Blocken, B., 2010. On the effect of wind direction and urban surroundings on natural
27 ventilation of a large semi-enclosed stadium. *Comput. Fluids* 39, 1146-1155.
- 28 Xie, X., Huang, Z., Wang, J., 2006. The impact of urban street layout on local atmospheric
29 environment. *Build. Environ.* 41, 1352-1363.
- 30 Yakhot, V., Orszag, S.A., 1986. Renormalization group analysis of turbulence: 1 Basic theory. *J. Sci.*
31 *Comput.*, 1, 1-51.
- 32 Zhang, Y.W., Gu, Z.L., Cheng, Y., Lee, S.C., 2011. Effect of real-time boundary wind conditions on
33 the air flow and pollutant dispersion in an urban street canyon – Large eddy simulations. *Atmos.*
34 *Environ.* 45, 3352-3359.